

*Full Length Research Paper*

# Modeling and application of permanent magnet synchronous generator (PMSG) based variable speed wind generation system

Sina Lotfi and Mahyar Sajedi\*

Department of Electrical Engineering, Ahar Branch, Islamic Azad University, Ahar, Iran.

Accepted 8 December, 2011

In the early development of wind energy, the majority of wind turbines were operated at constant speed. Recently, the number of variable-speed wind turbines installed in wind farms has increased and more wind turbine manufacturers are making variable-speed wind turbines. In this paper, maximum power control of wind turbine and permanent magnet synchronous generator connected with two back to back voltage source converters to grid are studied. Machine currents are controlled by indirect vector control method. In this method, generator side converter controls the maximum excitation (air gap flux) by machine's d-axis current and controls generator torque by machine's q-axis current. Permanent magnet synchronous generator (PMSG) speed is controlled by tip speed ratio upon the wind speed variations to generate the maximum output power. Grid side converter regulates the DC link voltage and injective active power by d-axis current and regulates the injective reactive power by q-axis current using simple control method P-Q. Simulation results depict that the proposed method operates properly.

**Key words:** Wind turbine, permanent magnet synchronous generator, maximum power control, superconductive inductor.

## INTRODUCTION

Nowadays, among all the renewable energy sources, wind systems are more economic in comparison with others. Variable wind speed systems deliver 20 to 30% more energy in comparison with the constant speed systems. They also decrease power oscillation and improve reactive power injection (Kim and Kim, 2007; Weisser and Garcia, 2005). Various technologies are developed for wind systems as their application has developed. During the previous years, permanent magnet synchronous generators (PMSGs) are greatly used in wind turbine applications because of their advantages such as low weight and velocity, high efficiency and gearless structure (Spooner and Williamson, 1996; Chinchilla

et al., 2006). Extracting maximum power of turbine and delivering an appropriate energy to grid are two important purposes in wind turbines. According to these purposes, AC-DC-AC structure is the best structure to convert the power in wind turbines (Spooner and Williamson, 1996; Chinchilla et al., 2006; Arifujaman et al., 2006; Hana et al., 2007; Sajedi et al., 2011). Figure 1 shows one of the most common structures applied for PMSGs. This structure contains a full wave diode rectifier, a DC-DC boost converter and a 3-phase inverter. In this structure, inverter satisfies the requirements related to grid connection and boost converter provides the ability of extracting maximum power using DC bus control in output of rectifier (Spooner and Williamson, 1996; Chinchilla et al., 2006).

The power extracted by the wind is related to the third order of wind speed. Applying power electronics

\*Corresponding author. E-mail: [Mahyar-sajedi@iau-ahar.ac.ir](mailto:Mahyar-sajedi@iau-ahar.ac.ir).

converters to transfer the power to grid with the possibility of speed variation in a great range of values is preferred because of their great advantages. Various methods are presented to control the maximum power where almost all of the efficient methods apply rotor speed feedback (Spooner and Williamson, 1996; Chinchilla et al., 2006; Senju et al., 2006). In this paper, maximum power point tracking is executed by sampling the rotor and wind speeds.

At first, it described how to estimate the speed and adaptive notch filter and then the controlling system of power injection to grid and maximum wind power extraction system are illustrated. Simulation results are shown at the end of this paper.

## MATERIALS AND METHODS

The proposed system consists of five main parts: Wind model, wind turbine, boost converter and superconductive inductor, power injection to grid, and maximum wind power extraction. These parts have been discussed and finally the simulation results have been introduced.

### Wind model

The model applied for this simulation is composed of three components and is described as follows (Surgevil and Akpinar, 2005):

$$V_{WIND} = V_{BASE} + V_{GUST} + V_{RAMP} \quad (1)$$

where  $V_{BASE}$  is the main component,  $V_{GUST}$  is the gust component and  $V_{RAMP}$  is the ramp component. The main component is a constant speed. Ramp component can be expressed by a sinusoidal function which is considered as a composition of several different sinusoidal functions and gust component is considered as storm and sudden wind.

### Wind turbine

The torque generated by wind blow is described by the following relations (Karrari et al, 2005):

$$\lambda = \frac{\omega_M R}{V_{WIND}} \quad (2)$$

$$P_M = \frac{1}{2} \rho \pi R^2 C_P V_{WIND}^3 \quad (3)$$

$$T_M = \frac{P_M}{\omega_M} = \frac{1}{2} \rho \pi R^5 C_P \frac{\omega_M^3}{\lambda^3} \quad (4)$$

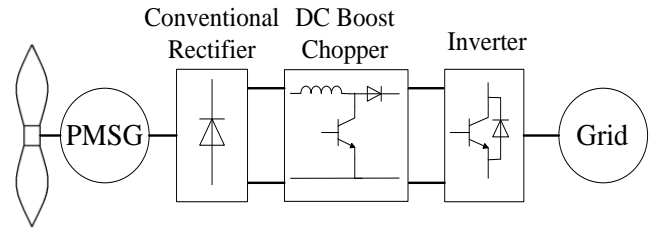


**Figure 1.** Wind turbine system with PMSG and boost converter.

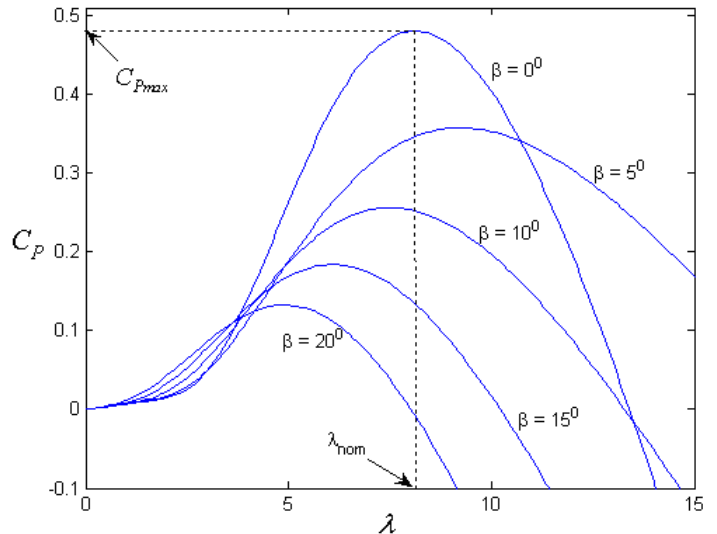


**Figure 2.**  $C_P$  in terms of  $\lambda$  for different  $\beta$  values.

where  $V_{WIND}$  is wind speed,  $R$  is the blades radius,  $P$  is the air density,  $\omega_M$  is rotor angular speed and  $\lambda$  is the tip speed ratio (TSR),  $C_P$  is the power conversion factor which can be defined as turbine power in proportion with wind power and is related to blades aerodynamic characteristics. Resulted mechanical torque is applied as the input torque to the wind generator and makes generator to operate. Power conversion factor is expressed as the function of tip speed ratio  $\lambda$  as follows:

$$C_P = (0.44 - 0.0167\beta) \sin \frac{\pi(\lambda-2)}{13-0.3\beta} - 0.00184(\lambda-2)\beta, \quad (5)$$

where  $B$  is blade's pitch angle. For a turbine with constant pitch,  $\beta$  is considered as a constant value (Figure 2),  $C_P$  variations in terms of  $\lambda$  for different  $\beta$  values. In this paper,  $\beta$  is considered zero where the  $c_p$  value would be 0.48. Table 1 shows the wind turbine parameters values applied in simulation.

**Table 1.** Wind turbine parameters.

Rated power	15 kW
Blade radius	5.5 m
Nominal wind speed	12 m/s
Minimum wind speed	4 m/s
Maximum wind speed	18 m/s
Blade pitch angle	0

### Boost converter and superconductive inductor

Boost converter stabilizes the voltage of DC link unrepentantly from the output voltage of rectifier which is caused by speed variation of synchronous generator. DC link voltage is stabilized through regulating the boost converter switch conduction ratio ( $D$ ).  $D$  is the result of dividing the conduction time of switch in each period by the switching period. Stabilized DC link voltage in the inverter terminals leads to efficiency increase and appropriate exploitation of power semiconductor devices. Boost converter behaves like a second order system which has an additional zero at the right side of imaginary axis. Right side zero makes system to operate like a non minimum phase system which is not desirable in voltage regulators; because of any variation in output voltage might increase before being corrected by the controller. As it is obvious in Figure 3, the energy storage device plays the main role in the operation of boost converter. During each switching period of DC converter and also during the conduction time of switch, energy is stored in magnetic field of inductor and then during the 2nd part of period where the switch does not conduct, energy is injected to the capacitor bank of DC link. If a superconductive inductor is used to exchange the electromagnetic energy, the ability of energy storing and the efficiency increases greatly. These energy storage devices are commonly applied to improve the dynamic behavior of power systems and to correct the oscillations of industrial loads. Especially when the system rating is not high, cost of using high temperature superconductors have been reduced obviously and the system has been economized nearly. In order to compare, it should be noted that what is presented in Nomura et al. (2005) is the application of systems with tens of  $MJ$  rating, but as what is proposed here, the storing devices limit the rating of the systems applied in boost converter to tens of  $KJ$ .

Natural frequency and damping ratio of boost converter are computed as follows (Ang and Oliva, 2005):

$$\xi = \sqrt{\frac{L}{C}} \frac{1}{2R(1-D)}, \omega_m = \frac{(1-D)}{\sqrt{LC}} \quad (6)$$

The aforementioned relation shows that a considerable increase in  $L$  value reduces the frequency of system and decreases the ripple components of state variables. On the other hand, as  $L$  value increases,  $\Delta I_L$  (current ripple of superconductive inductor) will decrease to the value in which the operation of controlling system will face with distortion. Thus, correct selection of superconductive inductor will lead to an economic system in addition to all advantages presented in Nomura et al. (2005).

### Power injection to grid

In Figure 3, inverter control system to control the injected active and

reactive powers is shown. The relations of these powers in synchronous reference frame are as follows (Nomura et al., 2005; Knight and Peters, 2005):

$$P = \frac{3}{2}(v_d i_d + v_q i_q) \quad (7)$$

$$Q = \frac{3}{2}(v_q i_d - v_d i_q) \quad (8)$$

If synchronous reference frame is synchronized with the grid voltage, the q-axis component of grid voltage will be zero and power relations will be as follows:

$$P = \frac{3}{2}v_d i_d \quad (9)$$

$$Q = -\frac{3}{2}v_d i_q \quad (10)$$

According to the aforementioned relation, by controlling the currents of d-axis and q-axis, active and reactive powers can be controlled respectively. Two controlling loops are used to control these currents. The outer loop of capacitor voltage control is used to generate the d-axis reference current. This control will end in transferring the total generated power to grid. Q-axis reference current is specified by desirably selecting the grid injected reactive power. If unit power factor is considered, this current would be regulated at zero value.

### MAXIMUM WIND POWER EXTRACTION

Figure 4 shows the relation between the output power of turbine and its speed for different wind speeds. It is seen that the optimum rotor speed is different in various wind speeds to obtain the maximum power of turbine. In PMSG, the relation between torque and inducted voltage is as follows:

$$T = K_t I_a \quad (11)$$

$$E = K_e \omega \quad (12)$$

where  $\omega$  is the angular rotor speed and  $I_a$  is stator current. On the other hand, it is obvious that:

$$E^2 = V^2 + (I_a \omega L_s)^2 \quad (13)$$

where  $V$  is the terminal phase voltage and  $L_s$  is the inductance of generator. DC voltage at the output of rectifier ( $V_{DC}$ ) is as follows:

$$V_{DC} = \frac{3\sqrt{6}}{\pi} V \quad (14)$$

which  $V_{DC}$  according to the relations (11) to (14) is as follows:

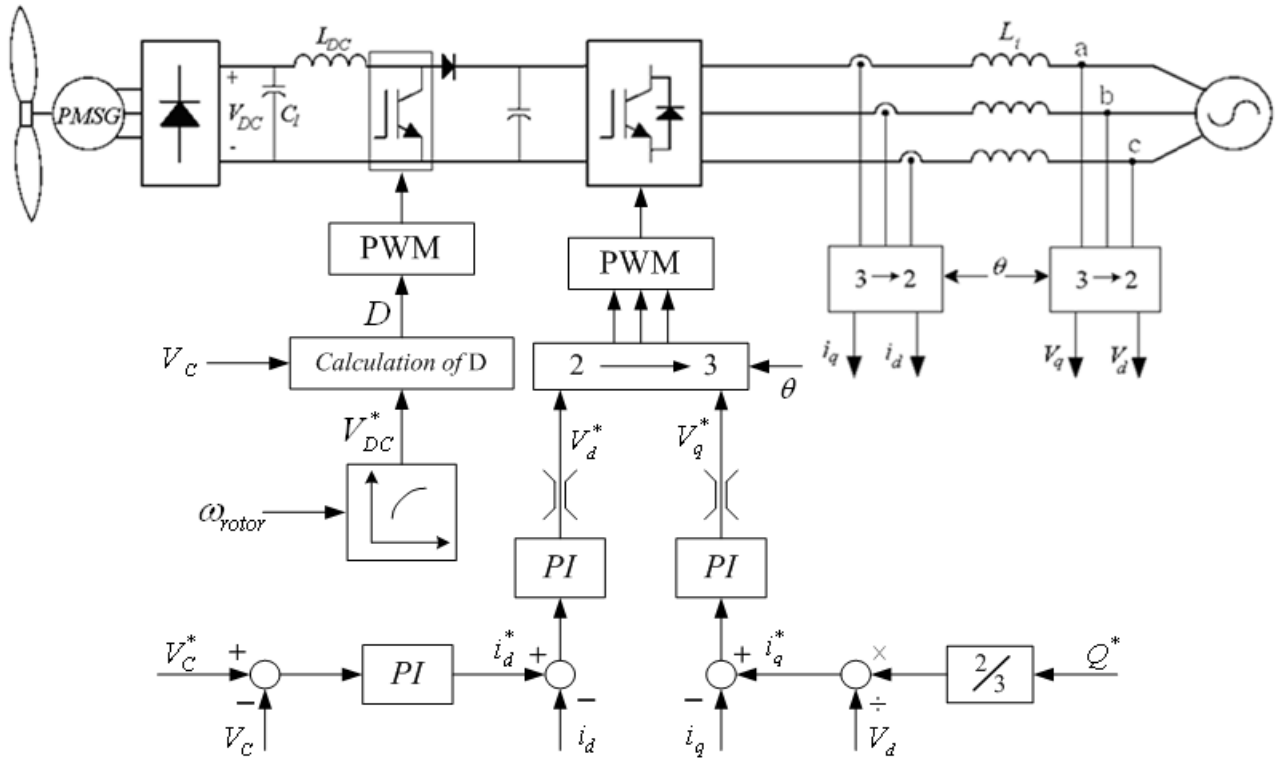


**Figure 3.** Configuration and control system of proposed wind energy system.

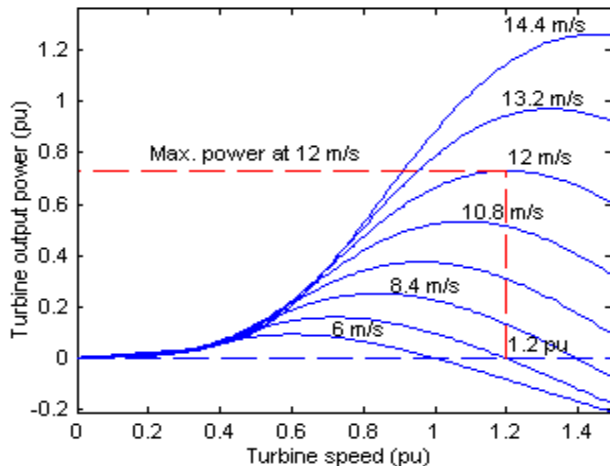


**Figure 4.** Maximum power of turbine in terms of wind and rotor speed.

$$V_{DC} = \frac{3\sqrt{6}}{\pi} \omega \sqrt{K_e^2 - \left(\frac{TL_s}{K_t}\right)^2} \quad (15)$$

In respect to the fact that the torque is determined by the rotor and wind speeds, a specific voltage value is estimated for a specific rotor and wind speed as relation (15).

If DC voltage relation is obtained in terms of optimum speed, resulted diagram would be as Figure 5. Now, a feedback from rotor speed, DC bus voltage can be obtained through Figure 5 and can be applied to the system. By applying this control, speed and voltage vary continuously until they reach their balance mode in a point on the curve as shown in Figure 5. In this case, maximum power of wind energy is obtained from the wind turbine.

As it is obvious, Figure 5 is a nonlinear curve. But it can easily be applied using a linear approximation around the nominal operation point. In this paper, a second order approximation is used. Determining optimum DC voltage and switching ratio of boost converter ( $D$ ) is calculated to reach this voltage.

$$D = \frac{V_c - V_{DC-Ref}}{V_c} \quad (16)$$

## RESULTS AND DISCUSSION

In order to study the operation of proposed wind turbine, the mentioned system is simulated using MATLAB/SIMULINK software with the parameters of Tables 2 and 3. Table 4 shows the parameters of controllers.

Figure 5 shows the DC voltage curve in terms of optimum rotor speed. Mentioned curve is derived through simulating system in various wind and rotor speeds. The dotted line is a second order approximation

**Table 2.** PMSG parameters.

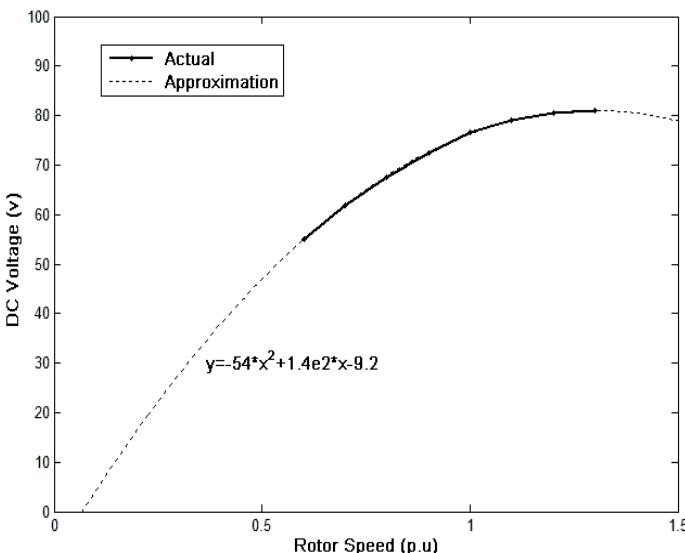
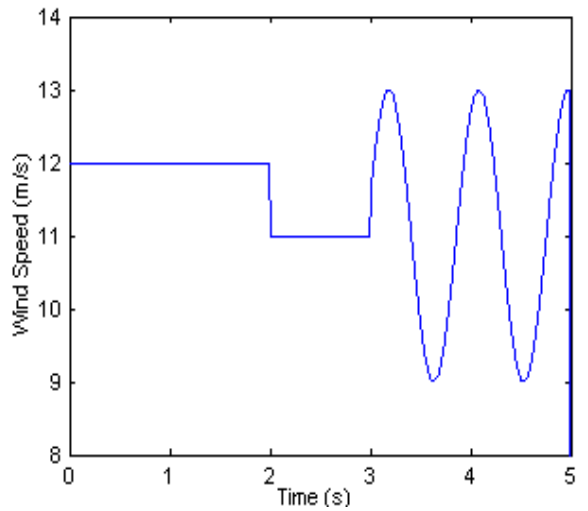
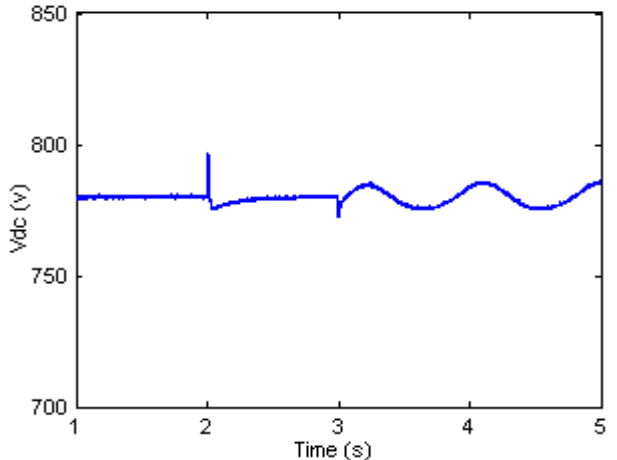
Parameter	Value
$R_s$	2.875 $\Omega$
$L_q$	8.5 mH
$L_d$	8.5 mH
$P$	4
$J$	0.0008 kg.m $^2$

**Table 3.** Simulation parameters

Parameter	Value
$V_i$	63.33 V
$L_i$	5 mH
LDC	2 mH
$C_1$	2200 $\mu$ F
$C_2$	2200 $\mu$ F
$f_s$	10 kHz

**Table 4.** Controllers parameters.

Parameter	Value
$K_{id}$	10
$K_{pd}$	1
$K_{iq}$	10
$K_{pq}$	1
$K_{ic}$	100
$K_{pc}$	1

**Figure 5.** DC voltage bus curve in term of optimum rotor speed obtained simulation and approximation.**Figure 6.** Simulated wind speed.**Figure 7.** Capacitor voltage.

of the aforementioned curve which is used to control the maximum power in coming simulations. Maximum and minimum rotor speeds are considered 1.3 and 0.6 p.u., respectively.

The proposed system is simulated for two seconds with variable wind speed as shown in Figure 6. In Figures 7 and 8, capacitor voltage and grid injected reactive power are shown respectively. These two figures show that the system has satisfied the requirements of grid connection appropriately, because the voltage level of capacitor is kept constant and reactive power transition is almost zero (unit power factor is considered here).

Figure 9 shows the electrical and mechanical power curves. It is obvious that after a short period of time, generated mechanical power of turbine tracks the maximum mechanical power of turbine (considering the wind

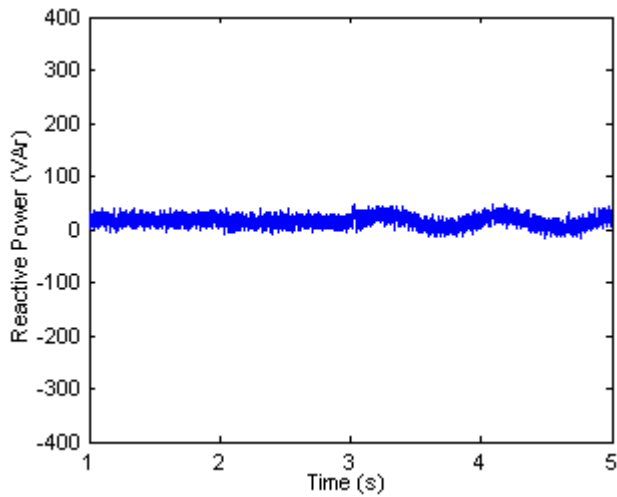


**Figure 8.** Injected reactive power to grid.

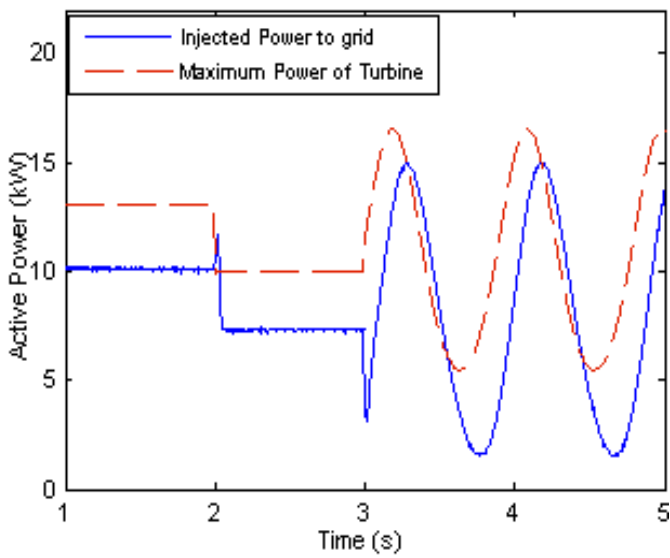


**Figure 9.** Injected active power to grid, maximum mechanical power of turbine.

speed). Also in Figure 9, grid injected active electrical power is shown which differs from the generated mechanical power according to the electrical and mechanical losses. As it is obvious, grid injected power curve tracks the maximum power curve of the turbine with about 0.1s delay time which is the result of using PI controllers in controlling circuit of inverter.

## Conclusion

As wind turbines develop, various technologies are

presented to improve their application. PMSG is under attention of these technologies because of its special abilities. In most PMSG wind systems, generated voltage of the generator is converted into DC voltage through a full-bridge diode rectifier and this voltage is controlled to control the maximum power of turbine. The grid side inverter is controlled by grid injected active and reactive power control method. Simulation results show that the maximum power is obtained from the turbines correctly for different wind speeds and active and reactive powers are injected to grid appropriately.

**Nomenclature:**  $V_{WIND}$ , wind speed (m/s);  $V_{BASE}$ , the main component of wind speed;  $V_{GUST}$ , the gust component of wind speed;  $V_{RAMP}$ , the ramp component of wind speed;  $\omega_M$ , rotor angular speed (rad/s);  $\lambda$ , the tip speed ratio (TSR);  $C_p$ , the power conversion factor;  $T_m$ , the mechanical torque applied to rotor;  $T_e$ , the generator electrical torque;  $\omega$ , the angular rotor speed (rad/s);  $I_a$ , stator current (A);  $\Delta I_L$ , current ripple of superconductive inductor;  $K_p$ , proportional PI controller value;  $K_i$ , integrated PI controller value;  $V_{DC}$ , DC voltage at the output of rectifier;  $V$ , the terminal phase voltage;  $L_s$ , the inductance of generator;  $D$ , switching ratio of boost converter.

## REFERENCES

- Ang S, Oliva A (2005). Power switching converters, CRC Press.
- Arifujaman M, Iqbal M, Quaicoe JE (2006). Maximum power extraction from a small wind turbine emulator using a dc-dc converter controlled by a microcontroller. *International Conference on Electrical and Computer Engineering*, pp. 213-216.
- Chinchilla M, Arnaltes S, Burgos JC (2006). Control of Permanent-Magnet Generators Applied to Variable-Speed Wind-Energy Systems Connected to the Grid. *IEEE Transaction on Energy Conversion*, 21(1): 130-135.
- Hana SG, Yua IK, Park M (2007). PSCAD/EMTDC-based simulation of wind power generation system. *Renewable Energy*, 32: 105-117.
- Karrari M, Rosehart W, Malik OP (2005). Comprehensive Control Strategy for a Variable Speed Cage Machine Wind Generation Unit. *IEEE Transaction on Energy Conversion*, 20(2): 415-423.
- Knight AM, Peters GE, (2005). Simple Wind Energy Controller for an Expanded Operating Range. *IEEE Transaction on Energy Conversion*, 20(2): 459-466.
- Nomura S, Ohata Y, Hagita T, Tsutsui H, Iio ST, Shimada S (2005). Wind farms linked by SMES systems. *IEEE Transaction on Applied Superconductivity*, 15(2): 1951-1954.
- Sajedi S, Kahlifeh F, Karimi T, Khalifeh Z (2011). Maximum power point tracking of variable speed wind energy conversion system. *Int. J. Phys. Sci.*, 6(30): 6843-6851.
- Senju T, Tamaki S, Urasaki N, Uezato K, Higa H, Funabashi T, Fujita H, Sekine H (2006). Wind velocity and rotor position sensorless

- maximum power point tracking control for wind generation system. *IEEE Power Electronics Specialists Conference*, 3: 2023-2028.
- Surgevil T, Akpinar E (2005). Modelling of a 5-kW wind energy conversion system with induction generator and comparison with experimental results. *Renewable Energy*, 30: 913–929.
- Spooner E, Williamson AC (1996). Direct coupled permanent magnet generators for wind turbine applications. *IEE Proceedings of Electric Power Applications*, 143(1): 1–8.
- Weisser D, Garcia RS (2005). Instantaneous wind energy penetration in isolated electricity grids: concepts and review. *Renewable Energy*, 30: 1299–1308.